APPLIED PHYSICS LETTERS **113**, 193702 (2018)

Probing drug-DNA interactions using super-resolution force spectroscopy

Haina Jia, Te-Wei Tsai, and Shoujun Xu[a)]
Department of Chemistry, University of Houston, Houston, Texas 77204, USA

(Received 24 June 2018; accepted 6 October 2018; published online 6 November 2018)

Atomic magnetometry and ultrasound, as individual techniques, have been used extensively in various physical, chemical, and biomedical fields. Their combined application, however, has been rare. We report that super-resolution force spectroscopy, which is based on the integration of the two techniques, can find unique biophysical applications in studying drug-DNA interactions. The precisely controlled ultrasound generates acoustic radiation force on the biological systems labeled with magnetic microparticles. A decrease in the magnetic signal, measured by an automated atomic magnetometer, indicates that the acoustic radiation force equals the binding force of the biological system. With 0.5 pN force resolution, we were able to precisely resolve three small molecules binding with two DNA sequences and quantitatively reveal the effect of a single hydrogen bond. Our results indicate that the increases in DNA binding force caused by drug binding correlate with the enthalpy instead of free energy, thus providing an alternative physical parameter for optimizing chemotherapeutic drugs. *Published by AIP Publishing*. https://doi.org/10.1063/1.5045787

Both atomic magnetometry and ultrasound are widely used techniques. Atomic magnetometers have been recently developed to be one of the most sensitive instruments for magnetic detection, rivaling superconducting quantum interference devices.[1–3] Subsequently, many applications have been demonstrated, ranging from fundamental physics, magnetic resonance imaging, nuclear magnetic resonance, to biomagnetism.[4–7] In particular, since magnetic particles are widely used in biochemical labeling, atomic magnetometers have been a valuable tool to detect biological molecules and intermolecular interactions.[8,9] Compared to optical-based spectroscopic techniques, however, atomic magnetometers are probably more difficult to use and less intuitive for providing specific molecular signatures. On the other hand, ultrasound radiation has been broadly employed in engineering, chemistry, and medicine.[10–12] In the presence of microparticles, ultrasound exerts substantial acoustic radiation force that can be used for particle manipulation and biological assays.[13–15] Recently, we showed super-resolution force spectroscopy (SURFS) that uses acoustic radiation force to precisely distinguish different intermolecular bonds, consequently revealing valuable mechanistic information of complex biological processes.[16,17]

Here, we report a unique application of SURFS in biophysics, as well as the critical technical aspects during the integration of an automated magnetometer and an ultrasound generator. The binding of three small ligands onto the minor grooves of two different DNA duplexes was precisely determined, with an order of magnitude better resolution than other force spectroscopic techniques. The structural difference of a single hydroxy group among drugs was also distinguishable. The automation of the magnetometer simplifies the experimental procedure and reduces operational error. These features combined will facilitate broad applications of SURFS in biophysics.

Figure 1 shows the schematic drawing of the overall apparatus, which includes a sample translation system, an ultrasound generator, and an atomic magnetometer. The sample was mounted on a glass rod driven by a linear motor. Ultrasound was generated by a piezo plate in conjunction with a function generator and an amplifier. The atomic magnetometer used high-vacuum cesium cells to minimize the operation temperature to 37 °C, which is advantageous for biological samples compared to other types of atomic magnetometers.[1,2] The sample was translated to the location of the piezo plate and subjected to ultrasound application. Then, it was moved inside the magnetic shield where its magnetic signal was determined by an atomic magnetometer. The process was repeated until the final ultrasound amplitude was reached. The smallest incremental step for the function generator was 0.002 V. We have confirmed that the sensitivity of the atomic magnetometer was not affected by the application of ultrasound, which was approximately 2.5 pT for 30 ms integration time with or without applying ultrasound (Fig. S1 in the supplementary material).

A key challenge for automated measurements is reproducibly generating acoustic radiation force without affecting the translation of the sample. We implemented a water reservoir, whose position was controlled by a translation stage, to be placed above the piezo plate. This allows constant coupling between the piezo and the sample, without restricting the translation of the sample required for magnetic measurements. To demonstrate automated measurements for hours, we designed a chemical system with a gradually decreasing magnetic signal, in which we used HCl to dissolve magnetic particles (details are provided in the supplementary material). Figure 2(a) shows the magnetic profiles of the sample in 5 min intervals. The top trace in black was the initial magnetic signal, measured by scanning the sample from outside the magnetic shield to the atomic sensor located at the center of the magnetic shield. The x-axis indicates the scanning distance. Each trace below the

[a)]Author to whom correspondence should be addressed: sxu7@uh.edu

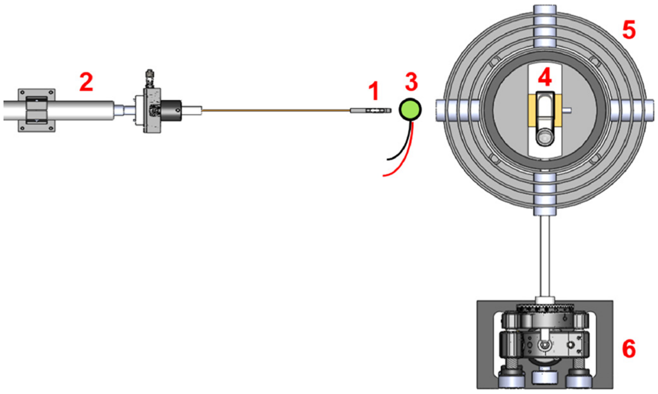

FIG. 1. Overview of the SURFS apparatus. *1*, sample; *2*, linear motor; *3*, piezo plate driven by amplified ultrasound; *4*, atomic sensor; *5*, magnetic shield; and *6*, mount of the atomic sensor.

black one was taken after reacting for every 5 min. The sample magnetic signal eventually reached a plateau. This was due to the residual magnetic field from the sample holder, which may be treated as a common background. The plot of the magnetic signal at different times is shown in Fig. 2(b). The profile followed single exponential decay, which was consistent with the first-order reaction because HCl was in excess. The half-life was 11.6 ± 0.6 min. This experiment showed that an automated atomic magnetometer coupled with ultrasound as the force source is feasible, which will eliminate the possible error caused by the manual sample loading and transferring steps between the centrifuge and atomic magnetometer in our previous work.[8]

To demonstrate biophysical applications of the integrated technique, we chose three representative ligands that bind the minor groove of DNA duplexes. Of the three,

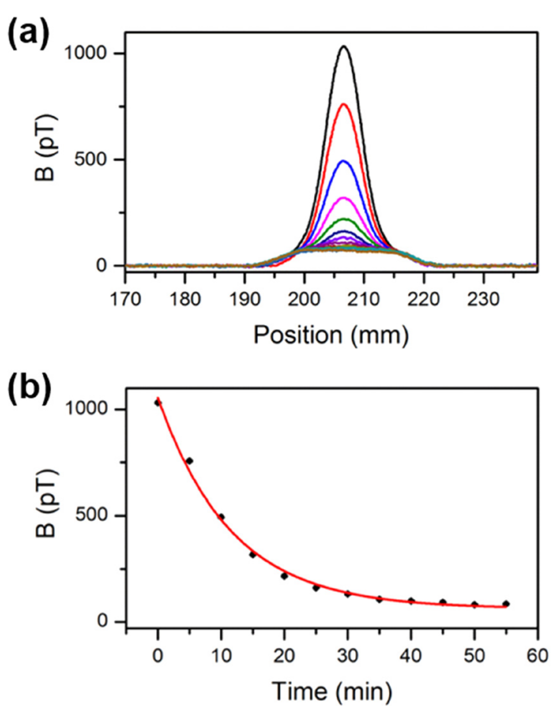

FIG. 2. Automated magnetic measurements for the dissolving reaction of magnetic particles in HCl. (a) Signal at various reaction times. From top to bottom: 5–55 min in 5 min intervals. (b) Plot of the magnetic signal vs. reaction time.

berenil and netropsin were well-known drugs that target DNA, and Hoechst 33258 (hereinafter referred to as Hoechst for simplicity) was commonly used for DNA staining.[18,19] Their molecular structures are shown in Fig. S2 in the supplementary material. Two different DNA sequences were selected based on the availability of binding thermodynamics for the ligands. The experimental procedures were similar to previous studies and are provided in the supplementary material.[17,20]

Figure 3(a) shows the relative magnetic signal vs. acoustic radiation force for a 11-basepair (bp) DNA containing a AAAAA segment for the three ligands. The DNA sequence was 5′-GCGAAAAACGC. The relative magnetic signals were obtained by dividing the magnetic signals at various acoustic radiation forces by the magnetic signal prior to applying ultrasound; each magnetic signal value was averaged from ten data points. A representative magnetic signal profile of berenil-DNA at 41 pN is shown in Fig. S3 in the supplementary material. The force values were obtained according to a previous calibration using a series of DNA duplexes, in which the same molecular systems were dissociated by both ultrasound and centrifugal force.[17] The calibration yielded the empirical formula of $F = 736 \times V^2 + 11$. Here, F is the acoustic radiation force in pN and V is the ultrasound amplitude in volts prior to amplification. The dissociation forces for the DNA alone, berenil-DNA, netropsin-DNA, Hoechst-DNA were 34.3, 41.3, 38.8, and 38.1 pN, respectively. The uncertainty was ± 0.5 pN (inset). To quantify the mechanical effect of drug binding, we define differential binding force, ΔF, which equals the dissociation force of the DNA with ligand binding subtracting it without the ligand. Therefore, berenil has the largest ΔF of 7.0 pN, followed by much smaller values of 4.5 and 3.8 pN for netropsin and Hoechst, respectively.

The advantage of SURFS is demonstrated by comparing the current results with force-induced remnant magnetization spectroscopy (FIRMS), a previous technique using centrifugal force instead of ultrasound.[8] FIRMS has a typical force resolution of ± 2 pN. The FIRMS results are shown in Fig. 3(b), in which the profile of Hoechst-DNA overlapped with that of DNA. This indicates that FIRMS was not able to distinguish Hoechst binding. A partial overlap was observed for netropsin-DNA. Only berenil-DNA was clearly resolved from DNA alone. Therefore, SURFS has a much better force resolution and is unique in distinguishing weak ligand-DNA binding.

The advantage of magnetic detection is shown by comparing with optical images obtained by a microscope (Amscope T650A, 10× objective). Two images were obtained, one before the dissociation of the DNA with no ultrasound and the other after using ultrasound at 0.25 V [Figs. 3(c) and 3(d)]. Counting the particles with ImageJ gave 2906 ± 74 for 0 V and 3009 ± 90 for 0.25 V.[21] The two values were the same within the uncertainty. This is because the magnetic particles remained on the surface after dissociation, resulting in no change in the particle count. In contrast, the magnetic dipoles of the dissociated particles became random due to the Brownian motion, resulting in a decrease in the magnetic signal that can be detected by the atomic magnetometer.

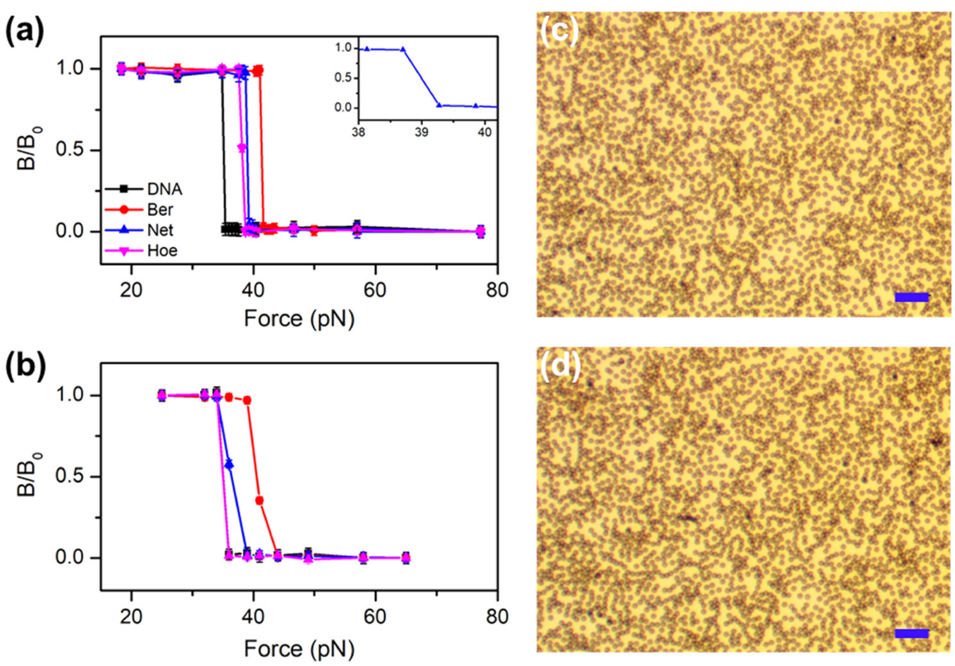

FIG. 3. Results of ligands binding a DNA duplex containing AAAAA. (a) SURFS results show a high force resolution. The inset shows the 0.5 pN force interval. (b) Lower-resolution results obtained by FIRMS. Note the overlap between DNA and Hoechst-DNA. (c) and (d) Microscopic images of the DNA sample before and after ultrasound, respectively. Ber: berenil; Net: netropsin; and Hoe: Hoechst 33258. Scale bar: 20 μm.

The precise force results by SURFS bring a different perspective in relating mechanical properties to thermodynamics. For the three ligands binding with the Poly(A)•Poly(T) duplex, berenil and Hoechst have similar ΔG, −9.4 and −9.5 kcal/mol, respectively, whereas ΔG for netropsin is a much more negative −12.4 kcal/mol.[22–24] Therefore, the mechanical difference measured with ΔF does not correlate with ΔG. Instead, the ΔH of the three ligands is −2.3, −0.4, and +8.6 kcal/mol, respectively. Comparing with the ΔF values of 7.0, 4.5, and 3.7 pN, respectively, we can conclude that ΔH appears to correlate with ΔF such that more negative values of ΔH are associated with higher values of ΔF.

To confirm the ΔF—ΔH correlation, we chose a DNA sequence that was identical to a literature report using calorimetry. The sequence was 5′-CGCGAATTCGCG. The SURFS results are shown in Fig. 4. The ΔF values are 1.7, 7.6, and 1.7 pN, for berenil, netropsin, and Hoechst, respectively. The force results suggest that only netropsin has significant negative ΔH binding to this DNA. This is consistent with the calorimetric results that ΔH for netropsin is −8.6 kcal/mol. For the other two ligands, ΔH is either close to zero or positive, with −1.3 kcal/mol for berenil and +7.5 kcal/mol for Hoechst.[25]

The high force resolution allowed us to study drug molecules with very similar structures. We chose daunomycin, doxorubicin, and epirubicin binding with a DNA duplex with sequences 5′-Biotin-GGA AAC CAA AGG and 5′-Biotin-CCT TTG GTT TCC. All three drugs are commonly used in chemotherapy,[26–29] with structures shown in Fig. S2 in the supplementary material. Among them, doxorubicin contains only one more OH group than daunomycin; doxorubicin and epirubicin differ only in chirality. The results are shown in Fig. 5. The binding force for the DNA duplex alone was 27.0 ± 0.5 pN; the force values for the drug-bound DNA were 41.3 ± 0.3, 49.1 ± 0.8, and 49.1 ± 0.8 pN, for daunomycin, doxorubicin, and epirubicin, respectively. These results led to ΔF of 14.3, 22.1, and 22.1 pN, respectively. Because the only structural difference between the last two and the first one was an OH group, we attributed the excess force increase of 7.8 pN to the additional hydrogen bond that was formed between the OH group and the DNA. In addition, for this particular DNA sequence, the chirality difference between doxorubicin and epirubicin did not affect their binding strength with the DNA. We are currently exploring other DNA sequences to identify if there will be a binding difference for the two drugs.

The significance of the SURFS applications in studying drug-DNA binding is twofold. One is regarding the binding thermodynamics. ΔH has been shown to be potentially a more relevant thermodynamic parameter for drug optimization than ΔG.[30] Establishing an alternative physical parameter for gauging ΔH is therefore valuable. Technically, ΔH is difficult to obtain. For example, optical-based techniques have yielded very different results compared to calorimetry because their only way for obtaining ΔH is using the van ’t Hoff equation. For the intrinsically narrow temperature range suitable for biological systems, this equation produces significant uncertainty.[25,31] Compared to calorimetry, our technique is easier to use, more specific, and cheaper. The other significance is the exceptional force resolution. Both

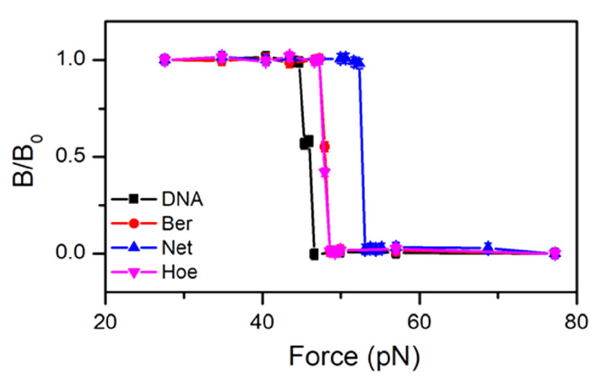

FIG. 4. SURFS results of the three ligands binding the DNA duplex containing AATT.

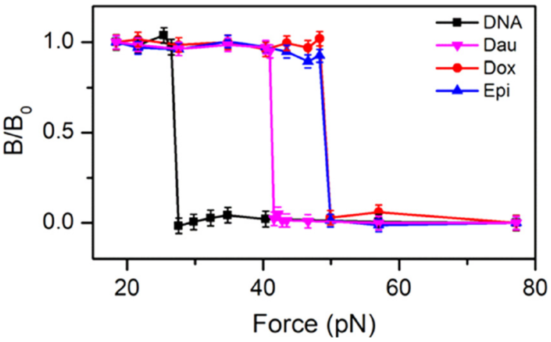

FIG. 5. SURFS results of daunomycin, doxorubicin, and epirubicin binding DNA. Note the profiles for doxorubicin and epirubicin overlap.

atomic force microscopy and optical tweezers have been used to study drug-DNA binding with important results.[32,33] However, the force distribution for both techniques is typically very broad because of their single-molecule nature. On the contrary, our atomic magnetometer measures 10^4–10^5 events simultaneously, leading to an improved force resolution that can resolve a single hydrogen bond.

A potential limitation for using acoustic radiation force is the power limit of the ultrasound. There are two effects that can damage the sample surface. One is cavitation that occurs at relatively high power. In the reported experiments, no cavitation was observed at even 0.5 V. In our previous work, we have shown that the power needed for dissociating longer DNA duplexes was approximately one order of magnitude below the cavitation threshold.[16] The other effect, the thermal effect, is more relevant to SURFS. We have measured the sample temperature vs. voltage and observed sample temperature increase at high voltages (Supporting Table). In order to limit the sample temperature to 37 °C, the voltage of the 1 MHz function needs to be below 0.40 V for the current apparatus. This translates to an upper force limit of 129 pN based on the calibration. We kept the voltage to be below 0.30 V in this work.

In conclusion, we expanded the application scope of atomic magnetometry and ultrasound in biophysics. The unique integration of the two fields gives both high sensitivity and resolution for molecular interactions. The resulting SURFS technique is potentially valuable for drug screening and represents an addition to the field of force spectroscopy.

See supplementary material for the experimental details, three supplementary figures, and one supplementary table.

This work was supported by the National Science Foundation (No. ECCS-1508845) and the National Institutes of Health (No. R01GM111452). S.X. acknowledges the partial support from the Texas Center for Superconductivity at the University of Houston (TcSUH).

[1]H. B. Dang, A. C. Maloof, and M. V. Romalis, Appl. Phys. Lett. **97**, 151110 (2010).
[2]V. Shah, S. Knappe, P. D. D. Schwindt, and J. Kitching, Nat. Photonics **1**, 649–652 (2007).
[3]D. Budker and M. V. Romalis, Nat. Phys. **3**, 227–234 (2007).
[4]D. F. J. Kimball, J. Dudley, Y. Li, and D. Patel, Phys. Rev. A **96**, 033823 (2017).
[5]I. M. Savukov, V. S. Zotev, P. L. Volegov, M. A. Espy, A. N. Matlashov, J. J. Gomez, and R. H. Kraus, Jr., J. Magn. Reson. **199**, 188–191 (2009).
[6]M. P. Ledbetter, I. M. Savukov, D. Budker, V. Shah, S. Knappe, J. Kitching, D. J. Michalak, S.-J. Xu, and A. Pines, Proc. Natl. Acad. Sci. U. S. A. **105**, 2286–2290 (2008).
[7]H. Xia, B.-A. Baranga, D. Hoffman, and M. V. Romalis, Appl. Phys. Lett. **89**, 211104 (2006).
[8]T.-W. Tsai, H. Yang, H. Yin, S.-J. Xu, and Y. Wang, ACS Chem. Biol. **12**, 1629–1635 (2017).
[9]L. Yao, Y. Li, T.-W. Tsai, S.-J. Xu, and Y. Wang, Angew. Chem., Int. Ed. **52**, 14041–14044 (2013).
[10]R. Kotzé and J. Wiklund, Meas. Sci. Technol. **25**, 105302 (2014).
[11]M. F. Mady, G. E. Awad, and K. B. Jørgensen, Eur. J. Med. Chem. **84**, 433–443 (2014).
[12]J. Provost, C. Papadacci, J. E. Arango, M. Imbault, M. Fink, J.-L. Gennisson, M. Tanter, and M. Pernot, Phys. Med. Biol. **59**, L1–L13 (2014).
[13]A. R. Mohapatra, S. Sepehrirahnama, and K. M. Lim, Phys. Rev. E **97**, 053105 (2018).
[14]M. Settnes and H. Bruus, Phys. Rev. E **85**, 016327 (2012).
[15]M. Wiklund and H. M. Hertz, Lab Chip **6**, 1279–1292 (2006).
[16]L. De Silva, L. Yao, and S.-J. Xu, Chem. Commun. **50**, 10786–10789 (2014).
[17]H. Jia, Y. Wang, and S.-J. Xu, Chem. Commun. **54**, 5883–5886 (2018).
[18]M. Wang, Y. Yu, C. Liang, A. Lu, and G. Zhang, Int. J. Mol. Sci. **17**, 779 (2016).
[19]J. Sheng, J. Gan, and Z. Huang, Med. Res. Rev. **33**, 1119–1173 (2013).
[20]Q. Hu and S.-J. Xu, Angew. Chem., Int. Ed. **53**, 14135–14138 (2014).
[21]C. A. Schneider, W. S. Rasband, and K. W. Eliceiri, Nat. Methods **9**, 671–675 (2012).
[22]D. S. Pilch, M. A. Kirolos, X. Liu, G. E. Plum, and K. J. Breslauer, Biochemistry **34**, 9962–9976 (1995).
[23]L. A. Marky, Biochemistry **28**, 9982–9988 (1989).
[24]F. G. Loontiens, L. W. McLaughlin, S. Diekmann, and R. M. Clegg, Biochemistry **30**, 182–189 (1991).
[25]I. Haq, Arch. Biochem. Biophys. **403**, 1–15 (2002).
[26]B. Doughty, Y. Rao, S. W. Kazer, S. J. J. Kwok, N. J. Turro, and K. B. Eisenthal, J. Phys. Chem. **117**, 15285–15289 (2013).
[27]J. B. Chaires, Annu. Rev. Biophys. **37**, 135–151 (2008).
[28]E. F. Silva, R. F. Bazoni, E. B. Ramos, and M. S. Rocha, Biopolymers **107**, e22998 (2017).
[29]A. Erdem and M. Ozsoz, Anal. Chim. Acta **437**, 107–114 (2001).
[30]E. Freire, Drug Discovery Today **13**, 869–874 (2008).
[31]F. G. Loontiens, P. Regenfuss, A. Zechel, L. Dumortier, and R. M. Clegg, Biochemistry **29**, 9029–9039 (1990).
[32]T.-H. Nguyen, L. J. Steinbock, H.-J. Butt, M. Helm, and R. Berger, J. Am. Chem. Soc. **133**, 2025–2027 (2011).
[33]P. M. Yangyuoru, S. Dhakal, Z. Yu, D. Koirala, S. M. Mwongela, and H. Mao, Anal. Chem. **84**, 5298–5303 (2012).